SCALING BEHAVIOUR OF THE ACOUSTIC TRANSMISSION RESPONSE OF ROTLIEGEND SANDSTONE UNDER VARYING AMBIENT STRESS

E. DIEGO MERCERAT*, KEES WAPENAAR, JACOB FOKKEMA and MENNO DILLEN

Department of Applied Earth Sciences, Delft University of Technology, P.O. Box 5028, 2600 GA, Delft, The Netherlands.
Present Address: Department of Seismology, Institut de Physique du Globe, 4 Place Jussieu, 75005 Paris, France.

(Received September 1, 2001; revised version accepted November 9, 2001)

ABSTRACT

Mercerat, E.D., Wapenaar, C.P.A., Fokkema, J.T. and Dillen, M., 2002. Scaling behaviour of the acoustic transmission response of Rotliegend sandstone under varying ambient stress. In: Fokkema, J.T. and Wapenaar, C.P.A. (Eds.), Integrated 4D Seismics. *Journal of Seismic Exploration*, 11: 137-158.

Ultrasonic experiments carried out on Rotliegend reservoir sandstone samples have shown a specific stress-dependent behaviour of the transmission response. Apart from the well-known velocity increase as ambient stress increases, the amplitude and the time are scaled when the stress is changed from one value to another. Our hypothesis is that when stress changes, some mineralogical constituents of the rock may change their acoustic properties differently from other constituents. As a consequence, different scattering attenuation effects take place within the rock. The observed stress-dependent scaling behaviour can be a consequence of the latter phenomenon.

In order to quantify the scaling behaviour, two approaches are used. First, a heuristically derived model from the experimental data is tested on numerically simulated data. Next, an analytically derived model from a modified version of the O'Doherty-Anstey expression for the transmission response through finely layered media is also analyzed and tested both on numerically simulated and experimental data. Both scaling models present two scalar parameters that relate a wavelet recorded at a high ambient stress with another recorded at a relatively low stress. Estimating these parameters from measurements for a range of different ambient stresses gives valuable information about the stress-dependent behaviour of the reservoir rock.

KEY WORDS: scaling behaviour, scattering attenuation, Rotliegend sandstone, ultrasonic experiments, varying tri-axial stress.

0963-0651/02/$5.00

INTRODUCTION

Changes in production or injection rates in a reservoir cause changes in the ambient stress state to which reservoir rocks are subjected. In order to monitor the in-situ stress by means of a seismic method, a relation between velocity and amplitude of the seismic response and the varying ambient stress has to be found. As a result of varying stresses, some elastodynamic properties of the rock may be considerably altered. Therefore the relation between ambient stress changes and seismic attributes can be used as an effective tool for characterization and monitoring of oil and gas reservoirs.

In practice, it is not possible to perform controlled stress-dependent seismic experiments. Therefore ultrasonic laboratory experiments are carried out in different sedimentary rock samples using triaxial and uniaxial pressure machines. The question still remains whether the extrapolation from the ultrasonic scale (hundreds of kHz) to the seismic scale (tens of Hz) is possible.

The fact that propagation of elastic waves in rocks can be sensitive to the effective stress is already well known from numerous laboratory experiments. A common observation from ultrasonic stress experiments is that induced velocity changes in the stress direction become progressively smaller as stress increases, until an asymptotic value is reached (Wyllie et al., 1956; Nur and Simmons, 1969; Lo et al., 1986). Recent ultrasonic experiments have been performed at the Laboratory of Rock Mechanics, Department of Applied Earth Sciences, Delft University of Technology, in order to study elastic wave propagation through rocks subjected to stress (Cruts et al., 1995; den Boer et al., 1996; Swinnen, 1997; Dillen et al., 1999).

In this work, we focus on a specific behaviour of the acoustic transmission response through a reservoir rock. The objective is to find a possible physical explanation for that behaviour in terms of wave propagation through a medium with stress-dependent elastodynamic parameters. From laboratory experiments, it appeared that not only the arrival time is reduced as a result of increasing stress, but the width of the wavelet is reduced by approximately the same relative amount. In other words, the time-axis seems to be scaled by a single factor when the ambient stress is changed from one value to another. This behaviour was coined as *scaling behaviour*. Also an increase in the amplitude of the transmitted signal can be clearly seen when the ambient stress increases.

In a previous compilation report (Swinnen, 1997), one possible explanation of the phenomenon was discarded assigning the scaling behaviour to source related effects. Experiments were carried out using different sample sizes of the same rock. The acoustic transmissions for different travel-path lengths at the same ambient stress showed amplitude decay much higher than the

geometrical spreading of a point source. It was concluded that the scaling behaviour should be related with the medium through which the wave propagates, specifically with its internal structure and acoustic characteristics. Our research is based on the following hypothesis: as ambient stress changes, some mineralogical constituents of the rock matrix change their acoustic properties differently from other constituents. As a consequence, different scattering attenuation effects take place within the rock, and scaled transmission responses are obtained.

In the literature the transmission and reflection effect of several multilayered media has been discussed. In the precursor article by O'Doherty and Anstey (1971), the authors analyzed all the relevant factors that affect the amplitude of a transmission signal. Amongst others, they gave special attention to the effect of internal multiple reflections generated by relatively high impedance contrasts within layered sequences. These short-path multiples have significant effects both in attenuation and time delays relative to the expected time of a primary wave transmitted directly through the layered structure. Numerical calculations show that as more and more layers are considered, the primary itself is decreased by transmission losses until the propagating wavelet is purely multiple energy. This transformation from primary to multiples has been conceived as a filter. Since the cause of this filtering is the abundance of thin layers too fine for discrete resolution, or in other words, with thicknesses much less than typical seismic wavelengths, it was known as *stratigraphic filtering*. The terminology was first introduced by Spencer et al. (1977), and presently widespread used after the book by Shapiro and Hubral (1999).

The physical reason for this stratigraphic filtering is the multiple scattering by 1D inhomogeneities, i.e., a horizontally layered sequence. Despite 3D heterogeneous media are more suitable for modelling rock matrix structures, we have good reasons to start with simple layered models in order to test whether scattering attenuation effects are responsible for the scaling of the traces.
Layers are distinguished by many possible causes, such as composition, texture, internal structure and/or a combination of all of them. Also important are the presence of some preferable orientations related to depositional environments and alignment of microcracks or grain contacts, as well. It is clear that the response of these different mineralogical and/or structural constituents of the rock to large static stress will not be the same. Therefore the stratigraphic filtering becomes stress-dependent and this leads to a possible explanation for the observed scaling behaviour.

This paper is organized as follows. First, a description of the ultrasonic experiments is presented, with special emphasis on the rock type used, the pressure machines and the acoustic installation. The relevant results about the stress-dependent scaling behaviour are treated including a heuristically derived model (den Boer and Fokkema, 1996) to express the scaling relation in

mathematical terms. After that, from some assumptions on the matrix structure of the rock, we derive a new scaling relation using a modified version of the O'Doherty and Anstey (1971) formalism. We perform numerical tests of wave propagation through layered media in order to test the different scaling models. The results with synthetic data are quite satisfactory, thus they suggest the applicability of the scaling model to the experimental traces. We then carefully apply the scaling model to a pair of traces recorded at two different ambient stresses. Finally some conclusions on the stress sensitivity of effective acoustic parameters of the rock are stated.

EXPERIMENTAL SET-UP

Rock sample

The experiments were conducted with a Flechtinger sandstone which is an aeolian Upper Rotliegend Permian sandstone, obtained from the Sventesius Quarry near Magdeburg in Germany. This formation consists of massive cross-bedded aeolian dune sandstone of medium grain size (0.25-0.5 mm) and a high level of compaction. For a complete description of the rock characteristics, we refer the reader to den Boer et al. (1996) and Dillen (2000). The measured porosity ranges from 5% to 10%. A permeability of 3.44 mD and a rock density of 2.65 g/cm^3 was reported. The mineralogy consists of 60% quartz, 20% feldspar, and 20% rock fragments cemented with calcite. From previous ultrasonic experiments, a clear velocity anisotropy related to the layering was observed (Dillen, 2000). In our experiments, the samples have been mounted such that its layering is perpendicular to the vertical direction.

Pressure machines and acoustic installation

The experiments were performed in the Laboratory of Rock Mechanics, Department of Applied Earth Sciences, Delft University of Technology. A uni-axial and a tri-axial pressure machine were used depending on the objective of each experiment and the sample shape. When using prismatic shaped samples it is not possible to use the tri-axial pressure machine, designed exclusively for cubic shaped samples.

In the tri-axial pressure machine the force is computer-controlled built up independently in the three perpendicular directions up to 3500 kN. It is not possible to apply a controlled pore pressure since it is an open system. Each uni-axial part of the machine has a piston on one side and a pressure plate on the other side. The pressure plates used have a dimension of 200 $\times$ 200 mm^2. Therefore the maximum applicable stress was 87.5 MPa. Three ceramic piezo-electric transducers with a central frequency of 1 MHz were mounted in

each pressure plate. They were in direct contact with the sample and pressed, with the aid of a spring, with a constant force of 900 N on the block.

In the uni-axial pressure machine the force is built up in the vertical direction by an hydraulic pump controlled by the operator, thus giving less accurate pressure measurements. However, the pressure plates, transducers and springs used are the same as in the tri-axial case. The maximum applied force is 800 kN. Therefore the maximum applicable stress is 20 MPa.

Piezo-electric broad-band transducers are mounted in each pressure plate. They are compressional-wave transducers with a central frequency of 1 MHz (Panametrics V-103). The traces are recorded at a sample frequency of 10 MHz. The recording is computer controlled and the gain is set when the samples are brought under maximum pressure. The traces are filtered with a band-pass filter of 30 kHz and 2 MHz as low cut-off and high cut-off, respectively.

SCALING BEHAVIOUR

The experiments were carried out for a range of different ambient stresses. Fig. 1 shows the transmission responses for isotropic tri-axial stresses applied ranging from 2 MPa to 82 MPa in a cubic block of Rotliegend sandstone.

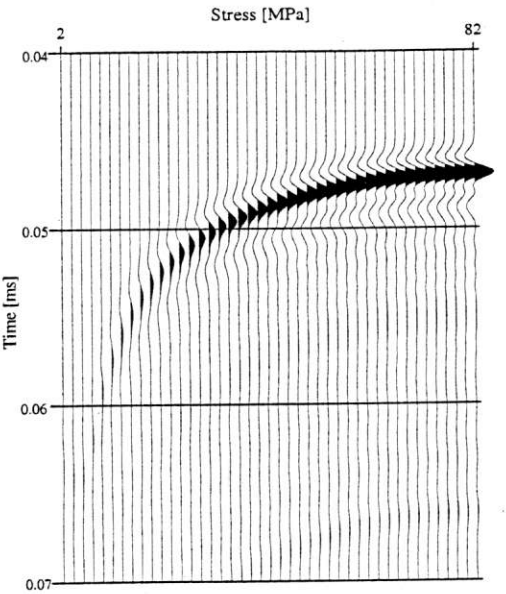

Fig. 1. Transmission responses (P-wave) of Rotliegend reservoir sandstone for varying tri-axial isotropic stress.

In order to study transmission responses at different travel-path lengths, the uni-axial pressure machine is used. The samples are mounted with the vertical axis (where the uni-axial stress is applied) perpendicular to the layering. Fig. 2 shows the transmission responses of two different sample sizes used: Rot11 (sample of 204 × 204 × 204 mm^3) and Rot23 (sample of 204 × 204 × 136 mm^3). The stress increases from left to right and it ranges from 2 MPa to 20 MPa, thus the difference between two adjacent traces is approximately 1 MPa. In Fig. 3 the transmission responses of Rot11 sample for vertically applied stresses ranging from 2 MPa (the latest arrival) to 20 MPa (the first arrival) in joint display.

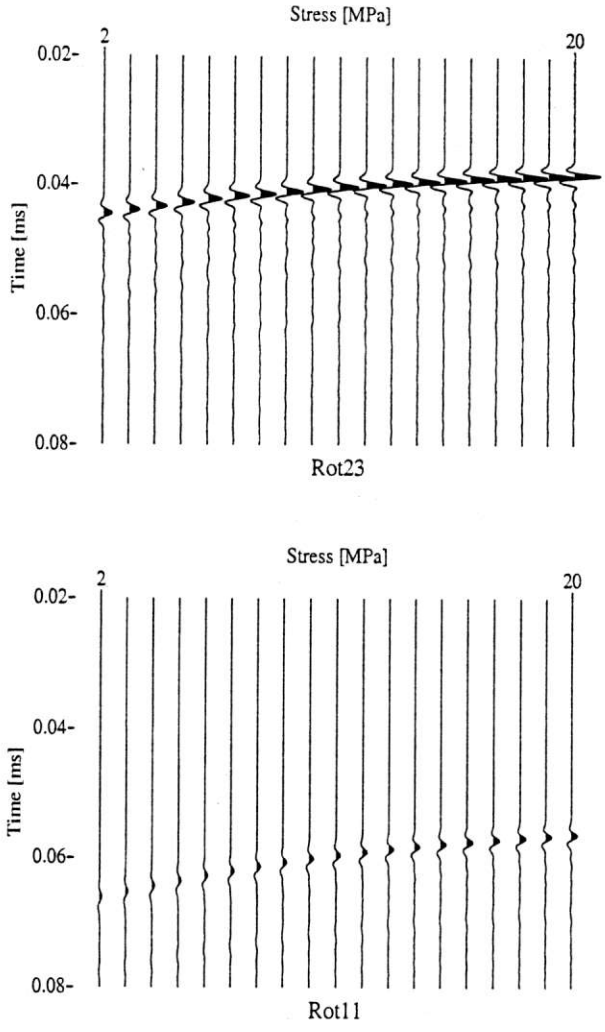

Fig. 2. Transmission responses (P-wave) of Rotliegend reservoir sandstone for varying uni-axial vertical stress. (Top) Rot23: 204 × 204 × 136 mm^3. (Bottom) Rot11: 204 × 204 × 204 mm^3.

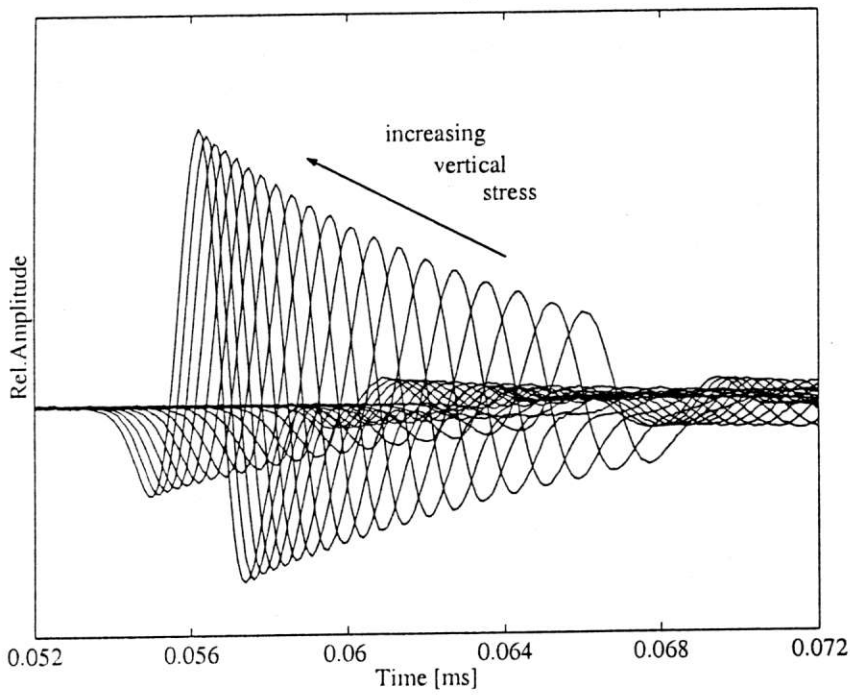

Fig. 3. Superposition on one time axis of transmission responses (P-wave) of Rot11 sample.

From both tri-axial and uni-axial experiments, it appeared that not only the arrival time reduces when the ambient pressure increases, but that the width of the wavelet reduces by approximately the same relative amount. In other words, the time-axis seems to be scaled by a single factor when the ambient pressure is changed from one value to another. Also the amplitude changes with changing stresses. It has been carefully checked (Swinnen, 1997) that these time and amplitude changes are not source effects, but that it is the propagation through the sandstone that changes with changing stress.

Heuristically derived scaling model

A simple scaling relation was derived from the experimental data by den Boer et al. (1996) and further studied by Swinnen (1997). A pair of recorded traces are approximately related by

$$p_B(t) = \beta p_A(t/\alpha) \quad , \tag{1}$$

where $p_B(t)$ and $p_A(t)$ denote the transmission responses at two different ambient stresses and α and β are the scaling parameters. The first one stretches the time axis with respect to $t = 0$, while the second one affects the wavelet amplitude. In the frequency domain, the scaling relation becomes

$$P_B(\omega) = \beta\alpha P_A(\alpha\omega) \quad , \tag{2}$$

where $P_B(t)$ and $P_A(t)$ are the Fourier transforms of $p_B(t)$ and $p_A(t)$, respectively. In order to calculate α and β, two traces are compared in the time domain, and using a normalized least-squares criterion, both scaling parameters are found by optimizing the match between the scaled trace with the recorded trace at a lower stress.

For example, Fig. 4 shows the transmission responses recorded at 10 MPa and at 6.4 MPa and a scaled version of the latter trace that approximately coincides with the former.

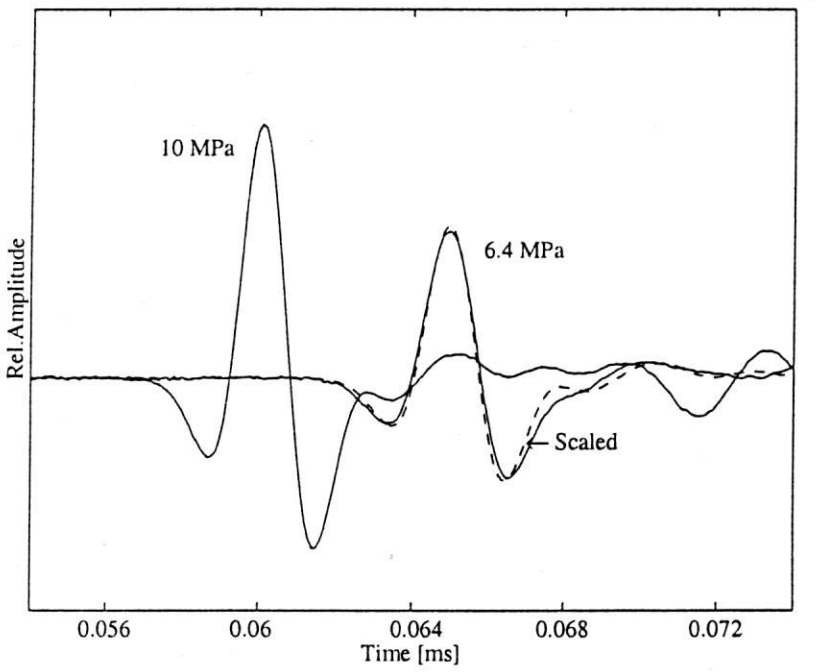

Fig. 4. Illustration of the scaling behaviour $p_B(t) = \beta p_A(t/\alpha)$. Trace recorded at 10 MPa (solid line, first arrival), trace recorded at 6.4 (solid line, second arrival) and scaled version (dashed line) from 10 MPa to 6.4 MPa.

THE BINARY LAYERED MEDIUM APPROACH

In the next two sections, we derive a new scaling model to relate a couple of traces recorded at two different stress states. It is based on some assumptions on the matrix structure of the sandstone and its reaction to the applied stress. We start by making a strong simplification, that is, we assume that the sandstone is horizontally layered. Although this is not very realistic, it is a suitable starting point for studying the scaling behaviour analytically. The second assumption is that the layered medium consists of only two types of material (hence the name binary layered medium); the layer thicknesses are in some way randomly distributed. The third assumption is that changes in the ambient stress do not affect the layer thicknesses, but only the material parameters. Fig. 5 exemplifies the assumed model for two different pressure states.

With these assumptions the depth-dependent normal-incidence plane-wave reflectivity r(z) obeys the following scaling relation

$$r_B(z) = \beta r_A(z) \quad , \tag{3}$$

where the subscripts A and B refer to two different ambient stress states. When the material parameters of both layer types react similarly (in a relative sense) to changes in the ambient pressure then $\beta = 1$; when they react differently, then $\beta \neq 1$. The average slowness $\bar{s}$ of the material obeys the following relation

$$\bar{s}_B = \alpha \bar{s}_A \quad . \tag{4}$$

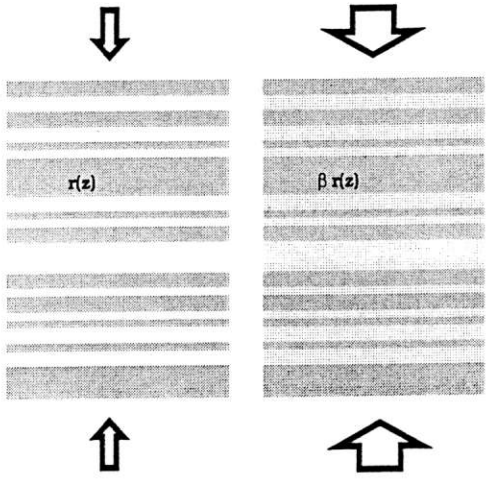

Fig. 5. Two different stress states in a binary layered medium. Left: state A (lower pressure). Right: state B (higher pressure).

It is beyond the scope of this paper to specify the scaling factors α and β and their mutual relation*. However, it is possible to state that if the stress state B is lower than stress state A, then α should be larger than 1. From the ultrasonic experiments and in accordance with equation (4), the lower the applied stress, the larger the average slowness of the rock (i.e., the smaller the average velocity). Apart from that, if stress states A and B do not differ too much, α and β should be close to 1. For our analysis it is sufficient to assume that relations (3) and (4) hold for some value of α and β. In the following section we will evaluate the scaling behaviour of the transmission response of binary layered media analytically.

SCALING BEHAVIOUR OF THE TRANSMISSION RESPONSE

The normal-incidence plane-wave transmission response of a layered medium can be expressed in the frequency domain in terms of a 'generalized primary' propagator $W_g(z_1,z_0,\omega)$, according to

$$W_g(z_1,z_0,\omega) = W_p(z_1,z_0,\omega)M(z_1,z_0,\omega)$$

$$= \exp\{-j\omega\bar{s}\Delta z\}\exp\{-A(2\omega\bar{s})\Delta z\} \quad , \tag{5}$$

where $\Delta z = z_1 - z_0$. The first exponential describes the (flux-normalized) primary propagation from depth level z_0 to z_1 and the second exponential accounts for the internal multiples generated at all interfaces between those two depth levels. The function A is the Fourier transform of the 'causal part' of $R(z)$, according to

$$A(k) = \int_0^\infty \exp\{-jkz\}R(z) \quad , \tag{6}$$

where $R(z)$ is the autocorrelation of the reflection function r(z), expressed by

$$R(z) = [1/(\Delta z - z)] \int_{z_0}^{z_1-z} r(\zeta)r(\zeta + z)d\zeta \quad . \tag{7}$$

Note that equation (5) is the well-known O'Doherty-Anstey relation (O'Doherty and Anstey, 1971), except that $A(k)$ in equation (6) is expressed in terms of a spatial rather than a temporal autocorrelation function. The depth-time conversion takes place in equation (5), where $A(k)$ is evaluated at $k = 2\omega\bar{s}$. Assuming r(z) obeys equation (3), $A(k)$ has the following scaling behaviour

* It is important to note that α and β in equations (3) and (4) are not the same as the scaling parameters in equation (1). However we prefer this notation because it is shown later that they play similar roles in both scaling models.

$$A_B(k) = \beta^2 A_A(k) \quad , \tag{8}$$

where the subscripts A and B refer again to two different ambient pressure states. For these two pressure states the generalized primary propagators read

$$\begin{aligned} W_{g,A}(z_1,z_0,\omega) &= W_{p,A}(z_1,z_0,\omega)M_A(z_1,z_0,\omega) \\ &= \exp\{-j\omega\bar{s}_A\Delta z\}\ \exp\{-A_A(2\omega\bar{s}_A)\Delta z\} \quad , \end{aligned} \tag{9}$$

$$\begin{aligned} W_{g,B}(z_1,z_0,\omega) &= W_{g,B}(z_1,z_0,\omega)M_B(z_1,z_0,\omega) \\ &= \exp\{-j\omega\bar{s}_B\Delta z\}\ \exp\{-A_B(2\omega\bar{s}_B)\Delta z\} \quad , \end{aligned} \tag{10}$$

or, using equations (4) and (8),

$$\begin{aligned} W_{g,B}(z_1,z_0,\omega) &= \exp\{-j\alpha\omega\bar{s}_A\Delta z\}\ \exp\{-\beta^2 A_A(2\alpha\omega\bar{s}_A)\Delta z\} \\ &= W_{p,A}(z_1,z_0,\alpha\omega)[M_A(z_1,z_0,\alpha\omega)]^{\beta^2} \quad . \end{aligned} \tag{11}$$

It is interesting to carefully compare equations (11) and (2), having in mind that the latter was derived from the real traces containing the source wavelet. In contrast, equation (11) has no information on the source function and it does represent the impulsive transmission response through the stack of layers. The similarities are clear: both of them contain the α parameter stretching the frequency axis, and the other parameter β controlling the amplitude. However, the β parameter in equation (2) accounts for the input wavelet amplitude, while β in equation (11) is merely related to an acoustic medium characteristic via equation (3).

NUMERICAL EXPERIMENTS

We are faced with two different scaling models for the transmission response. The former one [equation (1)] was heuristically derived analyzing the experimental data. The second one [equation (11)] was analytically derived from a modified O'Doherty-Anstey relation and making some assumptions on the pressure-dependent behaviour of the sandstone. We have performed numerical simulations for the transmission response through a binary layered medium, in order to check whether it is a convenient starting model for analyzing the stress-dependent rock behaviour.

The proposed sandstone model consists of a stack of horizontal acoustic layers with just two alternating velocities. The layer thicknesses are in some way randomly distributed and the density is considered constant and fixed for both material types. The assumption is that as the ambient pressure increases

one of the materials changes its velocity while the other remains fixed. Thus the reflectivity and the average slowness change according to equations (3) and (4).

The total transmission response is calculated by means of forward modelling of the acoustic wave equation in the frequency domain, using the so-called reflection method. Thus primary waves as well as internal multiple reflected waves are taken into account. We consider a plane-wave incident from the top and calculate the plane-wave transmitted to the bottom of the stack of horizontal parallel layers. After calculating the transmission impulse response, convolution with a Ricker wavelet (central frequency of 400 kHz) is carried out. This frequency is chosen in order to resemble the frequency content of the experimental traces (see Fig. 3).

The velocity ranges from 2500 m/s up to 3200 m/s for one material and it is fixed at 3500 m/s for the other material. Thus the wavelengths involved lie between 6.25 mm and 8.75 mm. We followed many authors who considered exponentially correlated heterogeneities as a good choice (Marion et al., 1994; Rio et al., 1996; Shapiro and Hubral, 1999) to obtain effective scattering attenuation. Thus the thickness of each bed is a random variable following an exponential distribution with mean $d = 0.6$ mm. Considering the wavelengths involved, these 1D heterogeneities can cause considerable scattering attenuation and dispersion of energy (Marion et al., 1994). The density is considered constant for both material types at 2.5 g/cm^3.

In Fig. 6, transmitted zero-phase Ricker wavelets through binary layered media are shown. The trace with the fastest arrival corresponds to the smallest impedance contrast and average slowness. The later arrivals are calculated by fixing one velocity at 3500 m/s and decreasing the other (from 3200 m/s to 2500 m/s), that is increasing the impedance contrast and the average slowness of the models. Note the similar scaling behaviour observed in the experimental data for different ambient pressures (Fig. 3).

The first, third and fifth arrivals in Fig. 6 are used to check both equation (1) and equation (11). The corresponding rock model parameters for these three cases are shown in Table 1.

Table 1. Binary layered model parameters.

	Total path	Mean thickness (d)	Velocity contrast
Model A			3200 m/s - 3500 m/s
Model B	20 cm	0.6 mm	3000 m/s - 3500 m/s
Model C			2800 m/s - 3500 m/s

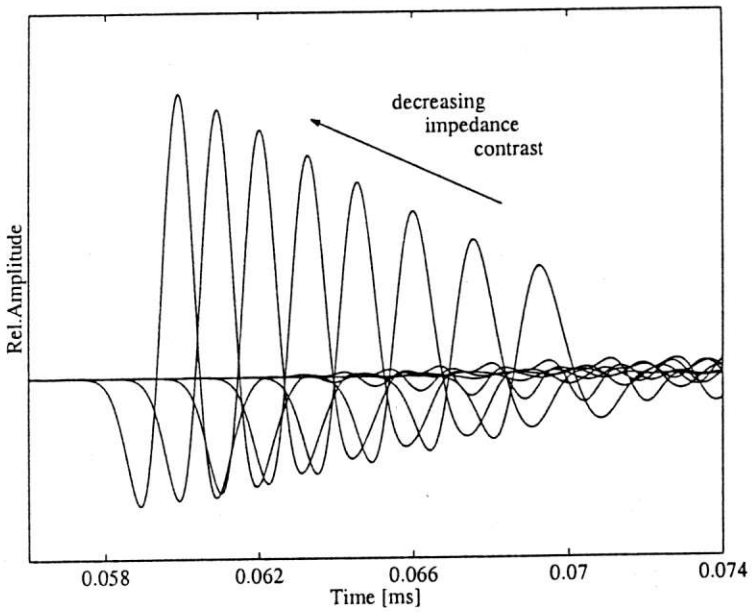

Fig. 6. Transmission responses (convolved with Ricker wavelet, 400 kHz central frequency) for varying impedance contrast: 3200 m/s -3500 m/s (leftmost arrival) to 2500 m/s -3500 m/s (rightmost arrival).

Even though the former scaling model was derived from real data, it does not give any explicit relation between the scaling parameters [α and β in equation (1)] and some physical characteristics of the reservoir rock. In spite of the latter, it is worthwhile to scale one trace from a low impedance contrast to a higher impedance contrast, applying the same least-squares technique previously used with the experimental data. The results can be seen in Fig. 7 and the scaling parameters in Table 2. Although the match is good, some differences in the amplitude of the main lobes and in the coda can be seen.

Table 2. Scaling parameters to scale trace A to B and C using both scaling models.

Model A	den Boer & Fokkema (1996)		New Scaling Model	
	α	β	α	β
Model B	1.036	0.870	1.035	1.718
Model C	1.078	0.692	1.075	2.481

On the other hand, the analytically derived scaling model of equation (11) presents scaling parameters somehow related to the acoustic characteristics of the layered model via equations (3) and (4). From the model velocities and using those equations, it is possible to calculate the scaling parameters shown in Table 2. They are used to scale the transmission response from model A to model B and C. It is interesting to note that the α parameters for both scaling models have similar values.

Before applying the scaling model, the direct path delay is removed from both responses according to the corresponding time delay for each model. This is done straightforwardly with the numerically simulated data as long as the primary travel time through the stack of layers is calculated exactly by our forward modelling routine. Thus equation (11) simplifies to

$$M_B(z_1,z_0,\omega) = [M_A(z_1,z_0,\alpha\omega)]^{\beta^2} \quad . \tag{12}$$

As follows from the latter formulation, the scaling model must be applied to the transmission impulse response, that is, with no source function included. As a first step in our forward modelling of the wave equation, the plane wave transmission response through the stack of layers is calculated. Then the scaling relation [equation (12)] is applied. Finally, the transmission impulse responses are convolved with a Ricker wavelet and shifted back to the correct arrival time.

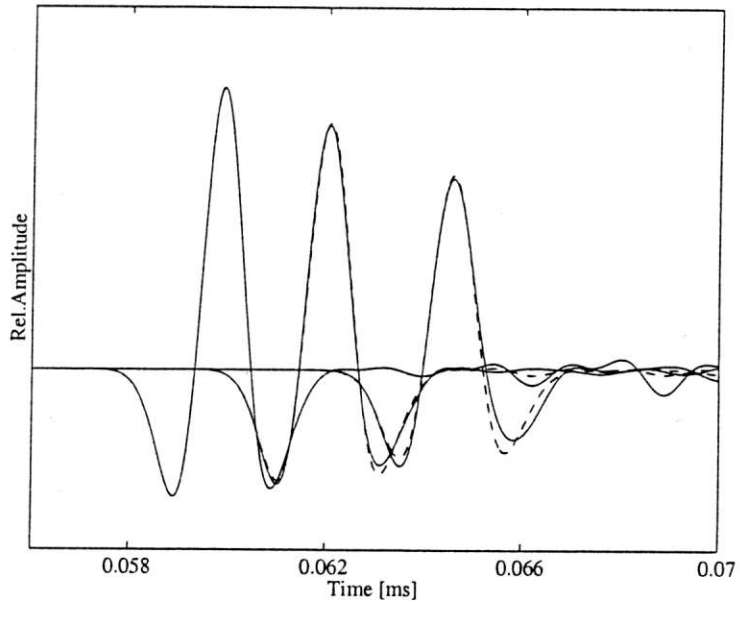

Fig. 7. First arrival (Model A), third arrival (Model B) and fifth arrival (Model C) of Fig. 6 (solid line), and scaled versions (dashed lines) from A to B and A to C using $w_B(t) = \beta w_A(t/\alpha)$.

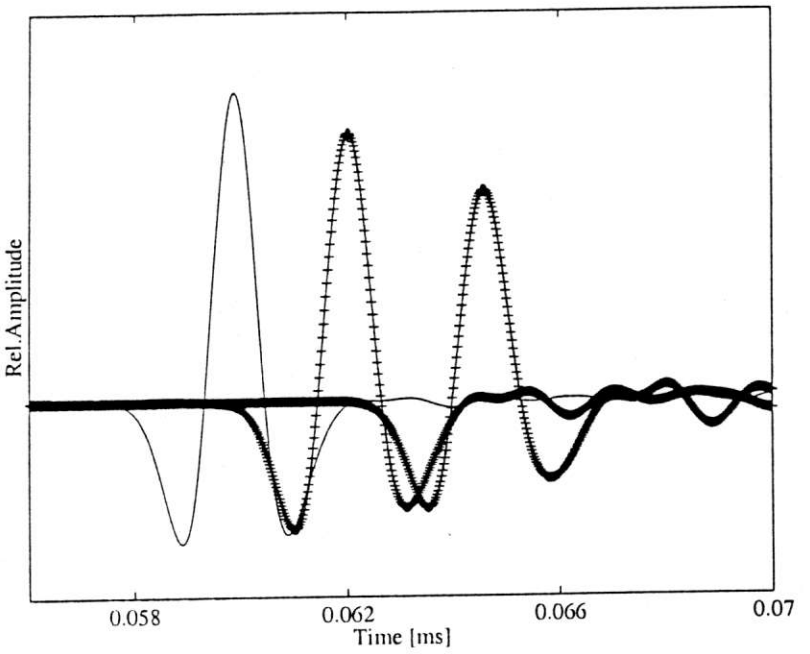

Fig. 8. Detail of the first, third and fifth traces (from the left) of Fig. 6 (solid lines) and scaled versions ('+' marked line) from the fastest arrival to the other two using equation (11).

In Fig. 8 the results are displayed. The match between the scaled version of the transmission response of model A and the transmission responses of models B and C are almost exact. This is another numerical confirmation of the O'Doherty-Anstey relation, although we know it is only an approximation to the total transmission response through a layered sequence.

STRESS-DEPENDENT SCALING BEHAVIOUR

After successfully testing the scaling model of equation (12) in the synthetic transmission responses, its application on the real data set looks promising. Specially because the estimation of the scaling parameters α and β can provide good insight in some acoustic properties of the rock subjected to stress. However, in our model we neglect in principle two facts: (a) the radiation pattern of the source (due to the plane wave assumption), and (b) the effect of any intrinsic losses that could have acted while the signals were travelling through the rock sample. The experiments were carried out on room-dry rock samples, thus reducing intrinsic absorption related to any fluid-flow mechanism.

The application of the previous scaling model of den Boer and Fokkema (1996) is straightforward with the real traces. A pair of traces must be chosen and applying the optimization technique previously described in this work, both scaling parameters can be found.

On the other hand the application of the analytically derived scaling model presented in this paper encompasses extra difficulties. The crucial one is the presence of the source wavelet in the real traces. The scaling model of equation (11) does not include the wavelet thus a wavelet deconvolution is necessary before its application. Our goal is based on the relation between medium parameters and scaling of the impulsive transmission response (i.e., Green function). Even under the assumption that one transducer emits always the same wave shape, the coupling between transducers and rock face may differ in each experiment. As a consequence the "input wavelet" may not be constant, even for the same rock type. The strategy is based on manipulating the transmission responses at the same ambient stress for different sample lengths.

The total transmission response (including the input wavelet) can be expressed for two different sample lengths as the product of the wavelet spectrum $S(\omega)$ and the generalized primary propagator of equation (5), according to

$$P(z_1,z_0,\omega) = S(\omega)W_p(z_1,z_0,\omega)M(z_1,z_0,\omega)$$

$$= S(\omega)\exp\{-j\omega\bar{s}\Delta z_1\}\exp\{-A(2\omega\bar{s})\Delta z_1\} \quad , \tag{13}$$

$$P(z_2,z_0,\omega) = S(\omega)W_p(z_2,z_0,\omega)M(z_2,z_0,\omega)$$

$$= S(\omega)\exp\{-j\omega\bar{s}\Delta z_2\}\exp\{-A(2\omega\bar{s})\Delta z_2\} \quad , \tag{14}$$

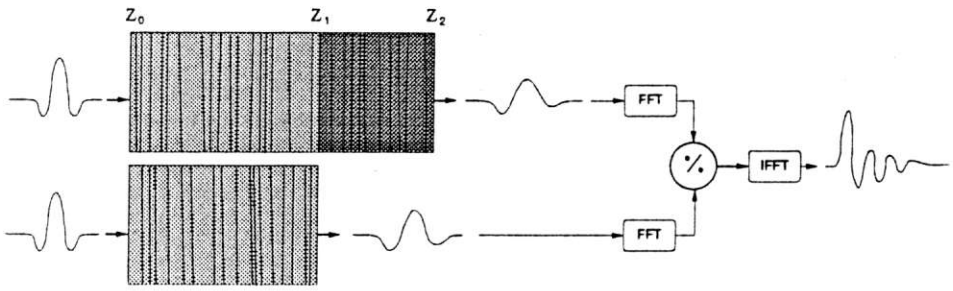

Fig. 9. Scheme of the strategy to calculate impulsive transmission responses (wavelet deconvolution) from the responses of two different rock sample sizes.

where $\Delta z_1 = z_1 - z_0$ and $\Delta z_2 = z_2 - z_0$. All the medium parameters are the same because the ambient pressure is the same. Dividing the response of equation (14) by that of equation (13),

$$W_g(z_2,z_1,\omega) = P(z_2,z_0,\omega)/P(z_1,z_0,\omega)$$

$$= \exp\{-j\omega\bar{s}(z_2 - z_1)\} \exp\{-A(2\omega\bar{s})(z_2 - z_1)\} \quad , \qquad (15)$$

the impulsive transmission response between z_1 and z_2 can be estimated (darker zone in Fig. 9). Repeating the same procedure for another pressure state, we are faced with a pair of deconvolved traces (i.e., source free) that can be scaled one onto the other.

SCALING EXAMPLE

In order to illustrate the previous technique, four transmission responses recorded at two different pressures and using two different sample sizes of Rotliegend sandstone are used (Rot11 and Rot23). The stress states are 10 MPa and 6.4 MPa. In Fig. 10 the four traces are visualized in joint display.

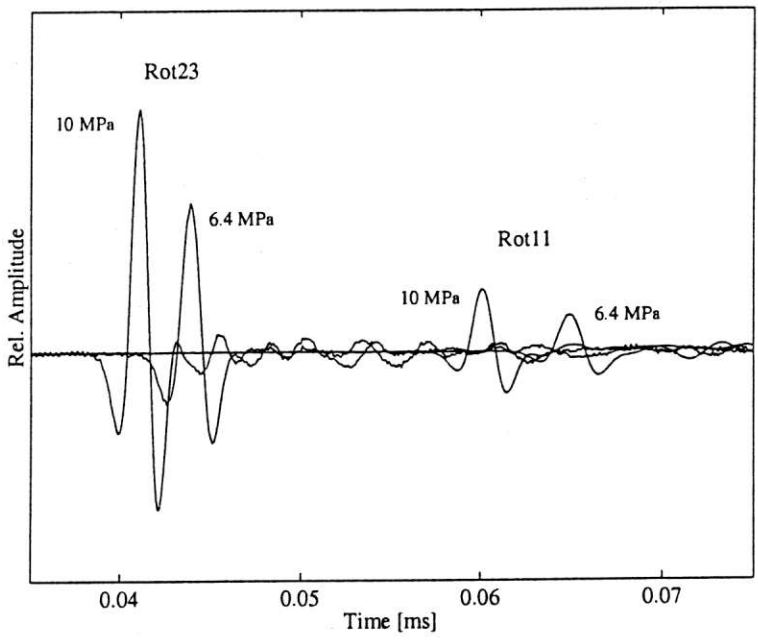

Fig. 10. Transmission responses for two samples of Rotliegend sandstone at two different pressures. Rot23: 204 × 204 × 136 mm³; Rot11: 204 × 204 × 204 mm³.

The scaling is performed in the frequency domain. Before submitting the traces to the Fourier transform, the wavelet has to be carefully tapered. We use a cosine tailed window of 200 samples (0.02 ms) starting 20 samples before the first break. After estimating the four spectra, the ratio of equation (16) is calculated using a stabilization constant $\epsilon = 10\%$ of the highest amplitude of $P(z_1,z_0,\omega)P^*(z_1,z_0,\omega)$ according to

$$W_g(z_2,z_1,\omega) = P(z_2,z_0,\omega)P^*(z_1,z_0,\omega)/[P(z_1,z_0,\omega)P^*(z_1,z_0,\omega)+\epsilon] \ , \qquad (16)$$

where * denotes complex conjugation. The deconvolution results for both stress states can be seen in Fig. 11.

In order to perform the scaling, it is necessary to shift first both traces to zero time [i.e., to cancel the first exponential in equation (9)]. In this manner we correctly apply the scaling model while avoiding any undesirable phase distortion. Unfortunately, when dealing with real traces, we have no information of the exact primary time delay (i.e., the first exponential in equation (11)], and how much of the observed time delay is caused by scattering within the rock.

We pick the first break of each arrival of Fig. 10 neglecting any time delay related to scattering. The picked arrival times are shown in Table 3. The primary time delay of one impulsive transmission response at one specific stress is simply the difference between the two picked arrival times for that stress.

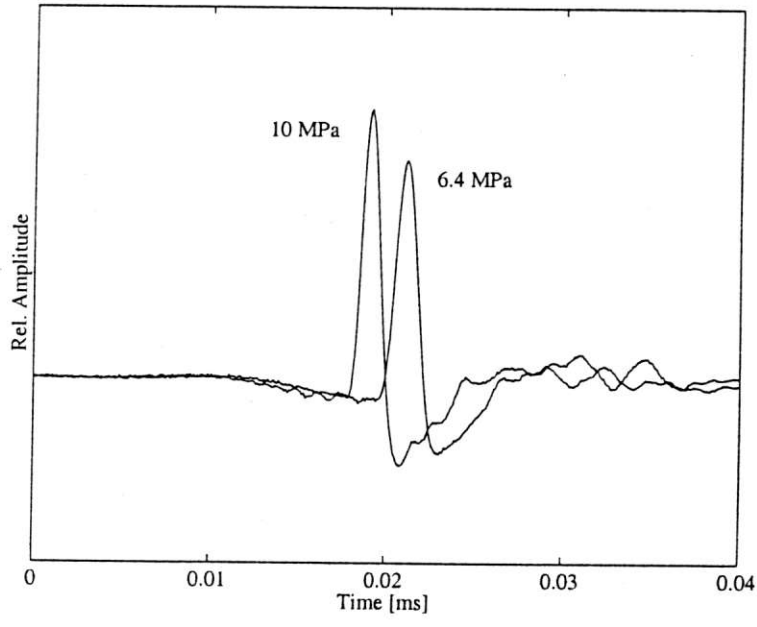

Fig. 11. Impulsive transmission responses at two different pressures estimated using equation (16).

Table 3. First break arrival times. Rotliegend sandstone.

Sample Label	Stress [MPa]	First break [ms]
Rot23	10.0	0.0385
	6.4	0.0412
Rot11	10.0	0.0570
	6.4	0.0616

Both impulsive transmission responses are then shifted to zero time. To be consistent with our choice of the primary time delays, equation (4) must be satisfied, thus the α parameter is somehow constrained. Therefore α is chosen equal to 1.103. After that, the 10 MPa response is scaled using equation (12) and the corresponding β is found to best fit the scaled trace with the 6.4 MPa response. In this case, β is found by inspection equal to 1.05. Finally, the traces are shifted back to their original times. In Fig. 12 a closer look of Fig. 11 and the scaled trace from the higher to the lower stress are shown.

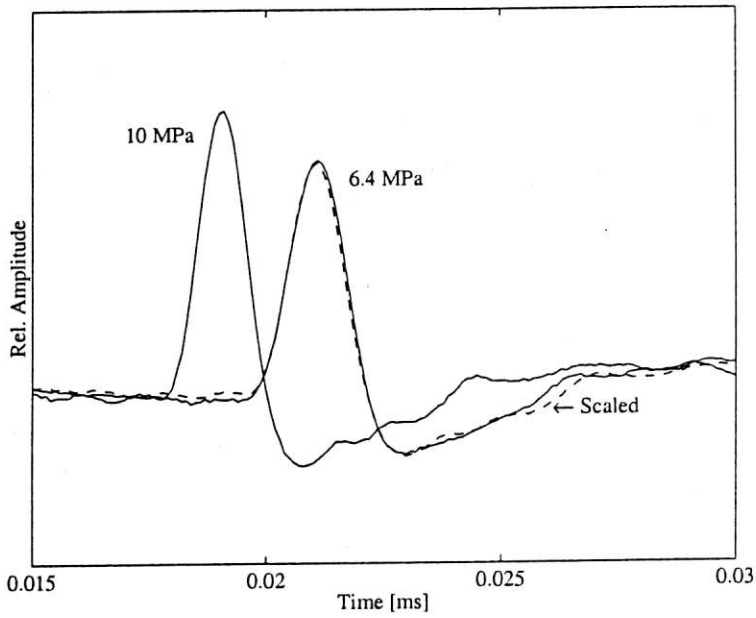

Fig. 12. Impulsive transmission responses at two different pressures and scaled version from 10 MPa to 6.4 MPa.

From the values $\alpha = 1.103$ and $\beta = 1.05$ and using equations (4) and (5), it can be inferred that the increase in vertical stress from 6.4 MPa to 10 MPa produces an increase in average velocity of 10% and a relatively small decrease in average impedance contrast of 5% in this specific Rotliegend sandstone.

CONCLUSIONS

In this paper, the relation between in-situ varying stress and acoustic parameters of a reservoir rock was analysed. Based on the experimental fact that the acoustic transmission responses are scaled as a function of the applied stress and on numerical simulations of wave propagation through rocks with stress-dependent elastodynamic parameters, we propose a possible physical explanation of the phenomenon. The dispersion of acoustic waves due to superposition of internal multiples may well be the cause of the scaling of the transmitted wavelets through a rock sample under varying ambient stress. The wavelet scaling produced by changes in the impedance contrast between layers corresponds to the pressure-dependent scaling behaviour observed in the experimental data. This correspondence suggests that as the ambient stress increases, the average slowness and the impedance contrast within the reservoir rock decrease.

Two different scaling models were analyzed. Both of them contain two scaling parameters to relate traces recorded at different ambient stresses. One of these parameters (α) stretches the time axis, and the other (β) controls the amplitude. The heuristically derived scaling model of equation (1) has been tested with numerically simulated data, giving reasonably good results. However, the relation between the scaling parameters and the acoustic characteristics of the rock is not explicit.

The analytically derived scaling model of equation (11) has been tested with numerical data, giving even better results than the previous one (compare Figs. 7 and 8). This result was expected since the scaling relation was derived from a modified version of the well-known O'Doherty-Anstey relation. Our hypothesis is that as stress changes, some variation in the velocity of one constituent material occurs. The α and β parameters are directly related with acoustic characteristics of the layered model (i.e., reflectivity and average slowness).

Equation (11) quantifies the scaling behaviour of the transmission response. Note that in both terms at the right-hand side the frequency is scaled with the same factor α. This agrees with our earlier observation that the arrival time and the width of the wavelet scale by approximately the same amount when the ambient pressure is changed. The exponent β^2 in the second term accounts

for the amplitude change, but has an effect on the phase as well. Since this exponent is applied to a frequency-dependent term, there is not a simple scaling relation in the time-domain.

The application of the analytically derived scaling model to real data is not straightforward. A source wavelet deconvolution should be done in order to apply the model of equation (11). Therefore we have tested a strategy that consists of spectral ratios of traces recorded at different travel-path lengths but similar applied stresses. Although we have made a number of simplifying assumptions, it is worthwhile to use equation (11) as a first approximate model for observations like those in Fig. 3. Estimating the parameters α and β from that type of measurements for a range of different ambient stresses gives valuable information about the stress-dependent behaviour of the reservoir rock.

ACKNOWLEDGEMENTS

This research is financially supported by the DIOC programme 'Determination and prediction of the 3D movements of the earth's surface', Delft University of Technology, The Netherlands, as well as by the Dutch Technology Foundation (STW, grant DTN.3547).

REFERENCES

den Boer, E.G., Dillen, M.W.P., Duijndam, A.J.W. and Fokkema, J.T., 1996. The effect of stress on wave propagation in aeolian Rotliegend Sandstone. Extended Abstr., 58th EAGE Conf., Amsterdam: P071.

den Boer, E.G. and Fokkema, J.T., 1996. Scaling propagation phemonena as result of an externally applied isotropic stress on an aeolian Rotliegend Sandstone sample. Expanded Abstr., 66th Ann. Internat. SEG Mtg., Denver: 1703-1706.

Cruts, H.M.A., Groenenboom, J., Duijndam, A.J.W. and Fokkema, J.T, 1995. Experimental verification of stress-induced anisotropy. Expanded Abstr., 65th Ann. Internat. SEG Mtg., Houston: 894-897.

Dillen, M.W.P., 2000. Time-lapse seismic monitoring of subsurface stress dynamics. PhD. thesis, Delft University of Technology.

Dillen, M.W.P., Cruts, H.M.A., Groenenboom, J., Fokkema, J.T. and Duijndam, A.J.W., 1999. Ultrasonic velocity and shear-wave splitting behaviour of a Colton sandstone under a changing triaxial stress. Geophysics, 64: 1603-1607.

Lo, T., Coyner, K.B. and Toksöz, M.N., 1986. Experimental determination of elastic anisotropy of Berea sandstone, Chicopee shale, and Chelmsford granite. Geophysics, 51: 164-171.

Marion, D., Mukerji, T. and Mavko, G., 1994. Scale effects on velocity dispersion: from ray to effective medium theories in stratified media. Geophysics, 59: 1613-1619.

Nur, A. and Simmons, G., 1969. Stress-induced velocity anisotropy in rock: an experimental study. J. Geophys. Res., 74: 6667-6674.

O'Doherty, R.F. and Anstey, N.A., 1971. Reflections on amplitudes. Geophys. Prosp., 19: 430-458.

Rio, P., Mukerji, T., Mavko, G. and Marion, D., 1996. Velocity dispersion and upscaling in a laboratory-simulated VSP. Geophysics, 61: 584-593.

Shapiro, S.A. and Hubral, P., 1999. Elastic Waves in Random Media. Fundamentals of Seismic Stratigraphic Filtering. Springer-Verlag, Berlin-Heidelberg.

Spencer, T.W., Edwards, C.M. and Sonnad, J.R., 1977. Seismic wave attenuation in non-resolvable cyclic stratification. Geophysics, 42: 939-949.

Swinnen, G., 1997. The effect of stress on wave propagation in reservoir rocks. MSc. thesis, Department of Civil Engineering, Katholieke Universiteit Leuven.

Wyllie, M.R.J., Gregory, A.R. and Gardner, L.W., 1956. Elastic wave velocities in heterogeneous and porous media. Geophysics, 21: 41-70.